

Article

The Impact of Anatomical Characteristics on the Structural Integrity of Wood

Lukas Emmerich *, Georg Wülfig and Christian Brischke

Wood Biology and Wood Products, University of Goettingen, Buesgenweg 4, D-37077 Goettingen, Germany; georg.wuelfing@stud.uni-goettingen.de (G.W.); christian.brischke@uni-goettingen.de (C.B.)

* Correspondence: lukas.emmerich@uni-goettingen.de

Received: 8 February 2019; Accepted: 21 February 2019; Published: 24 February 2019



Abstract: The structural integrity of wood is closely related to its brittleness and thus to its suitability for numerous applications where dynamic loads, wear and abrasion occur. The structural integrity of wood is only vaguely correlated with its density, but affected by different chemical, physico-structural and anatomical characteristics, which are difficult to encompass as a whole. This study aimed to analyze the results from High-Energy Multiple Impact (HEMI) tests of a wide range of softwood and hardwood species with an average oven-dry wood density in a range between 0.25 and 0.99 g/cm³ and multifaceted anatomical features. Therefore, small clear specimens from a total of 40 different soft- and hardwood species were crushed in a heavy vibratory ball mill. The obtained particles were fractionated and used to calculate the ‘Resistance to Impact Milling (RIM)’ as a measure of the wood structural integrity. The differences in structural integrity and thus in brittleness were predominantly affected by anatomical characteristics. The size, density and distribution of vessels as well as the ray density of wood were found to have a significant impact on the structural integrity of hardwoods. The structural integrity of softwood was rather affected by the number of growth ring borders and the occurrence of resin canals. The density affected the Resistance to Impact Milling (RIM) of neither the softwoods nor the hardwoods.

Keywords: brittleness; density; dynamic strength; High-Energy Multiple Impact (HEMI)-test; Resistance to Impact Milling (RIM)

1. Introduction

Most elasto-mechanical and rheological properties of wood are closely related to wood density and are therefore rather easily predictable. However, the anatomical features of wood, which can be wood species-specific, further affect especially dynamic strength properties such as the impact bending strength and shock resistance [1–3]. For instance, the large earlywood pores in ring-porous hardwoods such as English oak (*Quercus robur* L.), Sweet chestnut (*Castanea sativa* L.), Black locust (*Robinia pseudoacacia* L.) or Wych elm (*Ulmus glabra* Huds.) can serve as predetermined breaking points. Further deviations from an ideal homogeneous xylem structure such as large rays in European beech (*Fagus sylvatica* L.) or Alder (here: false rays, *Alnus* spp.), distinct parenchyma bands in Bongossi (*Lophira alata* Banks ex C. F. Gaertn.) or agglomerates of resin canals in Red Meranti (*Shorea* spp.), also have the potential to either strengthen or reduce the structural integrity of wood.

Similarly, wood cell wall modification affects different mechanical properties including the wood hardness and abrasion resistance, but also its brittleness and consequently its structural integrity. This has been shown previously with the help of High-Energy Multiple Impact (HEMI)-tests, where small wood specimens are subjected to thousands of dynamic impacts by steel balls in the bowl of a heavy vibratory mill. The fragments obtained are analyzed afterwards [4]. For instance, the weakening of cell walls by heat during thermal modification processes, especially in the middle lamella region,

leads to a steady decrease in the structural integrity of wood with increasing treatment intensity. The HEMI-test has further been used to detect fungal decay by soft rot, brown rot and white rot fungi (even in very early stages), the effect of gamma radiation, wood densification, wood preservative impregnation, wax and oil treatments, and different chemical wood modification processes [5].

It has previously been shown that the Resistance to Impact Milling (RIM), which serves as a measure of wood's structural integrity is very insensitive to varying densities, natural ageing, and the occurrence of larger cracks [5]. Furthermore, the RIM varies only little within one wood species, as shown for Scots pine sapwood (*Pinus sylvestris* L.) samples from trees in six Northern European countries [6]. However, the results from previous studies indicated that the structural integrity determined in HEMI-tests is not well correlated with wood density, since further variables such as wood species-specific anatomical characteristics of the xylem tissue interfere with the effect of density [7].

Objective

The aim of this study was to analyze the results from HEMI-tests of a wide range of softwood and hardwood species with an average oven-dry wood density in a range between 0.25 and 0.99 g/cm³ and with multifaceted anatomical features.

2. Materials and Methods

One hundred replicate specimens of 10 (ax.) × 5 × 20 mm³ were prepared from a total of 40 different wood species and separated between sapwood and heartwood, as listed in Tables 1 and 2.

To determine the oven-dry density (ODD), $n = 10$ replicate specimens of 10 (ax.) × 5 × 20 mm³ per wood species were oven dried at 103 °C until a constant mass, weighed to the nearest 0.0001 g; the dimensions were then measured to the nearest 0.001 mm. The oven dry density was calculated according to the following equation:

$$\rho_0 = \frac{m_0}{V_0} [\text{g cm}^{-3}] \quad (1)$$

where:

ρ_0 is the oven-dry density, in g·cm⁻³;

m_0 is the oven-dry mass, in g;

V_0 is the oven-dry volume, in cm³.

Table 1. The oven-dry density (ODD), Resistance to Impact Milling (RIM), degree of integrity (I), and fine percentage (F) of different softwood species. The standard deviation (SD) is in parentheses.

Name ¹	Botanical Name	ODD [g cm ⁻³]		RIM [%]		I [%]		F [%]	
Scots pine sw	<i>Pinus sylvestris</i>	0.41	(0.02)	88.2	(0.9)	67.4	(1.1)	13.5	(1.1)
Scots pine hw		0.58	(0.04)	84.5	(0.8)	41.9	(3.1)	1.3	(0.4)
Radiata pine sw	<i>Pinus radiata</i>	0.43	(0.02)	88.8	(0.5)	55.4	(2.1)	0.0	(0.0)
Carribbean pine hw	<i>Pinus caribaea</i>	0.39	(0.04)	87.3	(0.4)	52.4	(1.8)	1.1	(0.3)
European Larch sw	<i>Larix decidua</i>	0.56	(0.02)	85.2	(0.4)	44.5	(2.2)	1.2	(0.3)
European Larch hw		0.51	(0.02)	80.8	(1.5)	35.5	(4.8)	4.1	(0.4)
Douglas fir sw	<i>Pseudotsuga menziesii</i>	0.63	(0.02)	86.3	(0.4)	45.6	(1.8)	0.2	(0.2)
Douglas fir hw		0.51	(0.02)	82.2	(0.5)	34.8	(1.3)	1.9	(0.3)
Norway spruce	<i>Picea abies</i>	0.43	(0.03)	82.9	(1.7)	35.9	(6.1)	1.5	(0.4)
Coastal fir	<i>Abies grandis</i>	0.40	(0.06)	80.6	(0.5)	26.5	(1.3)	1.4	(0.4)
Western hemlock	<i>Tsuga heterophylla</i>	0.42	(0.03)	83.8	(0.7)	40.0	(2.1)	1.6	(0.3)
Yew	<i>Taxus baccata</i>	0.60	(0.03)	84.5	(0.9)	43.9	(3.2)	1.9	(0.3)

¹ sw = sapwood, hw = heartwood; heartwood if not otherwise indicated.

Table 2. The oven-dry density (ODD), Resistance to Impact Milling (RIM), degree of integrity (I), and fine percentage (F) of different hardwood species. The standard deviation (SD) is in parentheses.

Name ¹	Botanical Name	ODD [g cm ⁻³]	RIM [%]	I [%]	F [%]
English oak sw	<i>Quercus robur</i>	0.49 (0.02)	83.3 (0.5)	44.2 (1.7)	3.7 (0.4)
English oak hw		0.59 (0.01)	87.3 (1.2)	59.0 (4.3)	3.3 (0.4)
Black locust	<i>Robinia pseudoacacia</i>	0.68 (0.05)	83.5 (1.2)	41.0 (3.9)	2.3 (0.2)
Sweet chestnut	<i>Castanea sativa</i>	0.50 (0.03)	78.1 (2.3)	36.0 (4.2)	7.9 (1.8)
Ash	<i>Fraxinus excelsior</i>	0.62 (0.02)	83.1 (0.8)	40.4 (2.6)	2.7 (0.3)
Locust	<i>Gleditsia sp.</i>	0.66 (0.02)	86.7 (1.1)	52.6 (3.4)	1.9 (0.4)
Common walnut	<i>Juglans regia</i>	0.63 (0.02)	85.2 (0.5)	49.8 (2.1)	2.9 (0.3)
Wild cherry	<i>Prunus avium</i>	0.55 (0.01)	86.7 (0.7)	53.0 (2.2)	2.0 (0.3)
Black cherry	<i>Prunus serotina</i>	0.64 (0.04)	87.7 (0.6)	54.9 (2.1)	1.4 (0.2)
Beech	<i>Fagus sylvatica</i>	0.66 (0.02)	88.0 (0.4)	55.9 (2.2)	1.4 (0.3)
Maple	<i>Acer sp.</i>	0.61 (0.01)	89.1 (0.6)	58.0 (2.3)	0.5 (0.1)
Lime	<i>Tilia sp.</i>	0.44 (0.01)	90.1 (0.8)	61.1 (2.6)	0.2 (0.3)
Birch	<i>Betula pendula</i>	0.57 (0.02)	87.9 (0.4)	54.2 (1.6)	0.8 (0.1)
Hazel	<i>Corylus avellana</i>	0.68 (0.02)	86.9 (1.0)	52.8 (3.9)	1.8 (0.2)
Boxwood	<i>Buxus sempervirens</i>	0.96 (0.01)	90.3 (0.9)	64.1 (3.7)	0.9 (0.0)
Poplar	<i>Populus nigra</i>	0.39 (0.02)	86.3 (0.3)	50.5 (0.9)	1.8 (0.3)
Alder	<i>Alnus glutinosa</i>	0.48 (0.01)	86.9 (0.9)	54.6 (3.3)	2.3 (0.5)
Kiri	<i>Paulownia tomentosa</i>	0.25 (0.02)	80.9 (1.5)	40.0 (4.0)	5.5 (0.9)
Shining gum	<i>Eucalyptus nitens</i>	0.74 (0.11)	83.2 (1.5)	46.7 (4.5)	4.6 (0.9)
Teak	<i>Tectona grandis</i>	0.63 (0.09)	84.1 (0.7)	48.0 (2.1)	3.9 (0.8)
Ipe	<i>Handroanthus sp.</i>	0.93 (0.02)	86.0 (0.5)	51.8 (1.2)	2.6 (0.7)
Merbau	<i>Intsia spp.</i>	0.74 (0.03)	68.1 (2.4)	27.9 (1.8)	18.6 (2.7)
Bangkirai	<i>Shorea laevis</i>	0.79 (0.05)	87.7 (0.7)	54.9 (1.9)	1.4 (0.4)
Balau	<i>Shorea spp.</i>	0.92 (0.03)	84.3 (1.1)	51.7 (2.8)	4.8 (1.0)
Bongossi	<i>Lophira alata</i>	0.97 (0.03)	85.9 (1.0)	51.9 (2.7)	2.8 (0.7)
Amaranth	<i>Peltogyne sp.</i>	0.88 (0.01)	88.6 (0.7)	57.9 (2.7)	1.1 (0.0)
Basralocus	<i>Dicorynia sp.</i>	0.81 (0.02)	84.8 (0.6)	50.9 (1.9)	4.0 (0.4)
Garapa	<i>Apuleia sp.</i>	0.76 (0.04)	86.7 (1.1)	53.0 (3.3)	2.1 (0.5)
Limba	<i>Terminalia superba</i>	0.50 (0.03)	83.2 (1.2)	45.1 (2.7)	4.1 (0.9)
Kambala	<i>Milicia sp.</i>	0.62 (0.03)	79.7 (0.7)	45.2 (2.7)	8.8 (0.4)
Massaranduba	<i>Manilkara bidentata</i>	0.99 (0.04)	85.9 (0.6)	53.2 (2.5)	3.2 (0.2)
Greenheart	<i>Chlorocardium rodiei</i>	0.96 (0.02)	85.9 (1.5)	49.9 (5.3)	2.1 (0.8)

¹ sw = sapwood, hw = heartwood.

Afterwards, selected density specimens were cut with a traversing microtome and used for digital reflected-light microscopy with a Keyence Digital microscope VHX 5000 (Keyence Corporation, Osaka, Japan). Cross section photographs were taken at a magnification of 30 \times , and the diameter of the earlywood vessels, the vessel density, and the wood ray density were determined at a magnification of 200 \times for both the soft- and hardwoods. For the tropical species, the listed anatomical features were determined at a magnification of 100 \times . Therefore, $n = 10$ replicate measurements were conducted per wood species to determine the ray density and vessel density. The earlywood vessel diameter was determined on $n = 30$ vessels.

Five times 20 specimens of 10 (ax.) \times 5 \times 20 mm³ were submitted to High-Energy Multiple Impact (HEMI)-tests. The development and optimization of the HEMI-test have been described by [4] and [8]. In the present study, the following procedure was applied: 20 oven-dried specimens were placed in the bowl (140 mm in diameter) of a heavy-impact ball mill (Herzog HSM 100-H; Herzog Maschinenfabrik, Osnabrück, Germany), together with one steel ball of 35 mm diameter for crushing the specimens. Three balls of 12 mm diameter and three of 6 mm diameter were added to avoid small fragments from hiding in the angles of the bowl, thus ensuring impact with smaller wood fragments. The bowl was shaken for 60 s at a rotary frequency of 23.3 s⁻¹ and a stroke of 12 mm. The fragments of the 20 specimens were fractionated on a slit sieve according to [9], with a slit width of 1 mm, using an

orbital shaker at an amplitude of 25 mm and a rotary frequency of 200 min⁻¹ for 2 min. The following values were calculated:

$$I = \frac{m_{20}}{m_{\text{all}}} \times 100 [\%] \quad (2)$$

where:

- I is the degree of integrity, in %;
- m_{20} is the oven-dry mass of the 20 biggest fragments, in g;
- m_{all} is the oven-dry mass of all the fragments, in g.

$$F = \frac{m_{\text{fragments}<1\text{mm}}}{m_{\text{all}}} \times 100 [\%] \quad (3)$$

where:

- F is the fine percentage, in %;
- $m_{\text{fragments}<1\text{mm}}$ is the oven-dry mass of fragments smaller than 1 mm, in g;
- m_{all} is the oven-dry mass of all the fragments, in g.

$$\text{RIM} = \frac{(I - 3 \times F) + 300}{400} [\%] \quad (4)$$

where:

- RIM is the Resistance to Impact Milling, in %;
- I is the degree of integrity, in %;
- F is the fine percentage, in %.

3. Results and Discussion

3.1. Structural Integrity

The Resistance to Impact Milling (RIM) varied between 68.1% (Merbau) and 90.3% (Boxwood). In contrast, the degree of integrity (I) varied significantly more, i.e., between 26.5% (Coastal fir) and 67.4% (Scots pine sapwood), as did the fine percentage (F): i.e., between 0.0% (Radiata pine) and 18.6% (Merbau). The data for the RIM, I, and F are summarized in Table 1 for the tested softwood species and in Table 2 for the hardwood species. Besides differences between the wood species, the three indicators showed differences in the variation within one species, here expressed as the standard deviation (SD). The highest variation was obtained for F, followed by I and RIM. This supports previous findings pointing out the benefit of using the combined measure RIM, which is of higher sensitivity to differences in the structural integrity paired with less scattering of data compared to I and F [4,7]. In total, the SD of the RIM was between 0.3% (Poplar) and 2.4% (Merbau), corresponding to coefficients of variation (COV) between 0.4% and 3.5%, which is very low compared to mechanical properties such as the bending or impact bending strength (e.g., [7]).

3.2. Impact of Oven-Dry Density on Structural Integrity

A clear relationship between the ODD and structural integrity did not become evident, as shown for all the examined wood species and separately for the softwoods, ring- and semi-ring-porous hardwoods and diffuse-porous hardwoods in Figure 1. The RIM seemed to be at least superposed by further parameters such as structural features and anatomical characteristics. This coincides with the data for the Ash, Scots pine and Beech previously reported by [8], who showed that the density and RIM were not even correlated within one wood species. More recently, [7] reported that the density and RIM were also poorly correlated when considering ten different wood species representing a range of ODD between 0.37 and 0.77 g/cm³. However, according to [7] the RIM was fairly well correlated with the impact bending strength (IBS, $R^2 = 0.67$) and modulus of rupture (MOR, $R^2 = 0.56$), as determined

on axially matched specimens, which indicates that these strength properties are also at least partly affected by similar anatomical characteristics as the RIM is.

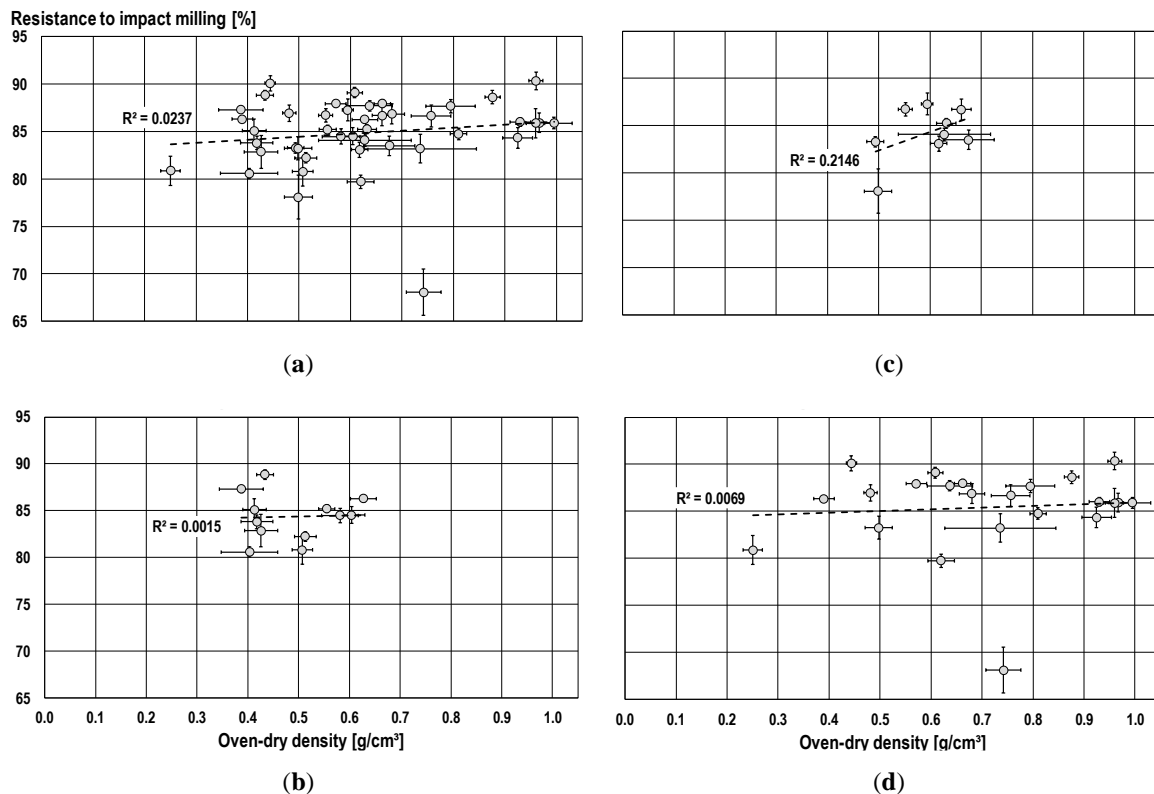


Figure 1. The relationship between the average oven-dry density and Resistance to Impact Milling (RIM): (a) all wood species ($y = 3.1629x + 82.887$); (b) softwoods ($y = 1.1035x + 83.791$); (c) ring- and semi-ring-porous hardwoods ($y = 19.634x + 72.545$); and (d) diffuse-porous hardwoods ($y = 1.8475x + 84.086$).

3.3. Impact of Anatomical Characteristics on Structural Integrity

The tested softwood species had a rather homogeneous and uniform anatomical appearance compared to the different hardwood species. However, even within this group the RIM varied between 80.6% and 88.8%. As summarized in Table 3, the softwood species differed also in the average tracheid diameter and in wood ray density. Nevertheless, the fracture patterns observed during the HEMI-tests were rather uniform, and fractures occurred predominantly along the growth ring borders in a tangential direction and along the wood rays and resin canals in a radial direction. The wood species showing an abrupt transition between the earlywood and latewood, such as the Larch and Scots pines, did not show a lower structural integrity compared to the species with a more gradual transition, such as the Norway spruce and Douglas fir, as one might expect due to a more sudden change of density within the tracheid tissue of one annual ring. Consequently, no fractures were observed along the transition line between the earlywood and latewood. In contrast to other softwood species, the Carribean and Radiata pines showed fractures in a tangential direction not only at the growth ring borders, but also where the resin canals ran in an axial direction.

As exemplarily shown for the heartwood of the Scots pine and Douglas fir in Figure 2, the major weak points, where fractures predominantly occurred, were the following: (a) the growth ring borders, where the less dense earlywood follows the dense latewood, and (b) the wood rays, which (1) consist of parenchyma cells, and (2) are running orthogonal to the main cell orientation in the tracheid tissue.

Table 3. The anatomical characteristics (tracheid diameter, ray density) and description of fractures during the HEMI-tests of different softwood species (standard deviation in parentheses).

Wood Species	Tracheid Ø [µm]		Wood Ray Density [mm ⁻¹]		Fracture Behaviour		Remarks
					tang.	rad.	
Scots pine sw	29	(6)	4.6	(1.2)	GR	RC	wider rings compared to hw
Scots pine hw	25	(5)	3.7	(1.5)	GR	RC	-
Radiata pine sw	22	(4)	4.4	(1.3)	GR	R, RC	-
Carribbean pine hw	28	(4)	5.2	(1.2)	GR	R, RC	-
European larch sw	35	(7)	5.9	(1.7)	GR	R	wider rings compared to hw
European larch hw	35	(6)	4.4	(1.1)	GR	R	-
Douglas fir sw	25	(6)	4.3	(1.2)	GR	R, RC	-
Douglas fir hw	23	(5)	3.9	(1.2)	GR	R	-
Norway spruce	25	(5)	4.5	(1.0)	GR	R	-
Coastal fir	28	(5)	5.7	(1.3)	GR	R	-
Western hemlock	25	(5)	5.0	(1.3)	GR	R	-
Yew	10	(3)	7.1	(1.4)	(GR)	(R)	Irregular fracture pattern

GR = along growth rings, R = along rays; RC = along resin canals; tang. = tangential growth direction; rad. = radial growth direction.

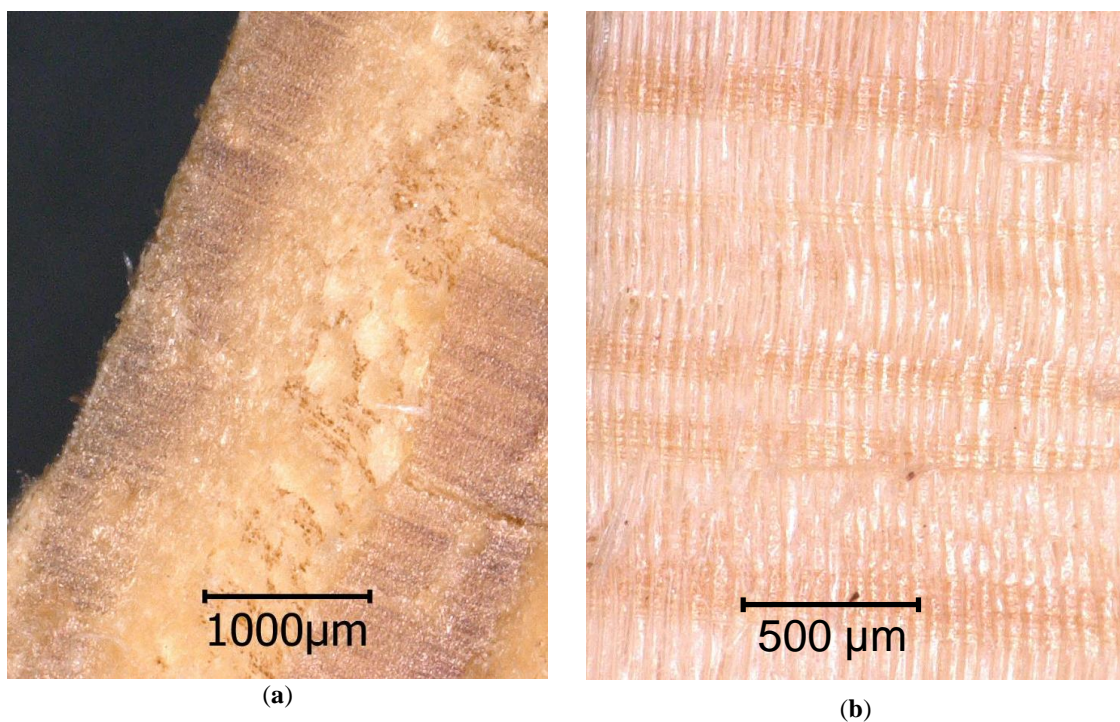


Figure 2. The fracture pattern in the softwoods: (a) Cross section of the Scots pine heartwood, fracture along a growth ring border; (b) The radial fracture section of the Douglas fir heartwood, fracture along the rays.

The fractures in the ring-porous hardwood species often followed the wide-luminous earlywood vessels, such as in the English oak, Sweet chestnut, Ash, Locust, and Black locust (Table 4). The specimens consequently broke apart in a tangential direction. In addition, the fractures occurred along the latewood vessel fields where high portions of paratracheal parenchyma were present (Figure 3). The ring-porous hardwoods with broad wood rays, such as the English oak, also showed fractures running parallel to the latter. Finally, the average diameters of the earlywood vessels were not correlated with the structural integrity, although, in the earlywood of all the ring-porous hardwoods, the fractures occurred preferentially in a tangential direction following the vessel rings.

Table 4. The anatomical characteristics (earlywood vessel diameter, vessel density, ray density) and description of fractures during the HEMI-tests of different hardwood species (standard deviation in parentheses).

Wood Species	Earlywood Vessel Ø		Vessel Density		Wood Ray Density		Fracture Behaviour ¹	
		[µm]		[mm ⁻²]		[mm ⁻¹]	tang.	rad.
English oak sw ²	247	(51)	7.7	(1.6)	8.4	(2.0)	EW	P
English oak hw	202	(49)	10.1	(2.0)	10.7	(1.8)	EW	P
Black locust	190	(40)	11.5	(1.0)	6.9	(1.1)	EW	R *
Sweet chestnut	209	(30)	7.7	(1.5)	11.8	(1.5)	EW	V-V
Ash ³	169	(21)	13.8	(1.7)	6.6	(0.8)	EW	n.a.
Locust	165	(25)	16.1	(2.0)	4.4	(1.2)	EW	R, P *
Common walnut	134	(32)	7.7	(2.0)	5.7	(1.3)	V-V	V-V
Wild cherry	33	(8)	171.6	(31.3)	6.1	(1.4)	GR	R
Black cherry ⁴	33	(9)	67.9	(22.9)	5.6	(1.3)	n.a.	R
European beech	40	(8)	131.9	(15.4)	3.0	(1.3)	GR *	n.a.
Maple ⁵	46	(7)	54.5	(3.4)	7.9	(1.7)	GR	R *
Lime ⁶	39	(9)	104.7	(14.0)	4.8	(1.1)	n.a.	n.a.
Birch	54	(13)	45.2	(8.5)	8.3	(2.4)	n.a.	R
Hazel	28	(6)	98.9	(20.2)	11.6	(2.5)	GR	n.a.
Boxwood ⁶	10	(4)	213.9	(14.0)	11.0	(2.5)	n.a.	R *
Poplar ⁷	58	(13)	33.7	(6.4)	11.0	(1.5)	n.a.	R
Alder	41	(10)	108.0	(16.7)	11.7	(2.0)	GR *	R
Kiri	164	(55)	5.2	(2.0)	2.4	(0.8)	V-V	V-V, R *
Shining gum ²	144	(25)	7.6	(3.2)	11.3	(1.1)	V-V	V-V
Teak ⁸	184	(57)	6.3	(1.7)	4.1	(0.7)	V-V	R *
Ipé ²	103	(9)	23.2	(2.7)	7.8	(0.9)	P *	V-V
Merbau	250	(40)	4.0	(1.4)	4.2	(0.9)	V-V, P *	V-V, P *
Bangkirai	207	(32)	7.3	(1.7)	3.7	(1.3)	P	V-V, R *
Balau	137	(13)	11.9	(2.9)	9.1	(1.2)	P	V-V, R *
Bongossi	232	(41)	2.9	(1.1)	9.9	(1.2)	P	V-V, P *
Amaranth	109	(16)	4.4	(1.7)	6.9	(1.7)	P, V *	R
Basralocus ²	190	(33)	2.8	(1.0)	7.9	(1.0)	P *	V-V
Garapa	121	(19)	15.2	(3.0)	8.3	(1.3)	P	V-V
Limba	139	(28)	4.4	(1.7)	10.2	(1.0)	n.a.	R
Kambala	193	(41)	2.8	(0.8)	4.4	(1.0)	(P)	R
Massaranduba	113	(18)	13.1	(3.3)	10.5	(1.5)	(P)	R
Greenheart ²	90	(16)	14.0	(2.0)	7.5	(0.9)	n.a.	V-V

¹ n.a. = not available (no clear pattern evident), GR = along growth rings, R = along rays, RC = along resin canals, EW = along earlywood vessels, P = in parenchyma tissue, V-V = vessel to vessel, V = at vessels, * = characteristic plays minor role; remarks related to fracture patterns: ² radial, parallel to rays; ³ no clear radial pattern; ⁴ very often parallel to rays; ⁵ parallel to growth rings; ⁶ irregular fracture pattern; ⁷ samples often compressed; ⁸ often at growth ring border.

This stands to some extent in contrast to findings by [2], who studied the perpendicular-to-grain properties of eight North-American hardwood species and found that the earlywood vessel area fraction negatively influenced the radial maximum stress and strain, whereas the ray width and area fraction were positively related to the maximum radial properties. The rays also affected the transverse stiffness significantly.

Studies conducted by [10] showed that wood rays have a positive effect on the tensile strength of English oak and European ash wood. However, as shown for the fragments obtained in the HEMI-tests, the latewood vessel fields turned out to be weak spots when it comes to dynamic loads in different anatomical directions. Therefore, the potentially positive effect of the wood rays on the structural integrity might be superposed by other anatomical features.

Finally, the RIM of the heartwood of the English oak (87.3%) was significantly higher than that of its sapwood (83.3%), which is to some extent surprising since sapwood is often considered to be less brittle than heartwood [11]. While the fine percentage (F) of both English oak materials was almost equal, the degree of integrity (I) of the heartwood was remarkably higher than that of the

sapwood, which might be related to the potential 'gluing' effects of the tylosis which were present in the earlywood vessels in the heartwood (Figure 3b), but were absent in the sapwood. Whether and to what extent the formation of tylosis has a positive effect on structural integrity would need to be further investigated using different generally tylosis-forming wood species.

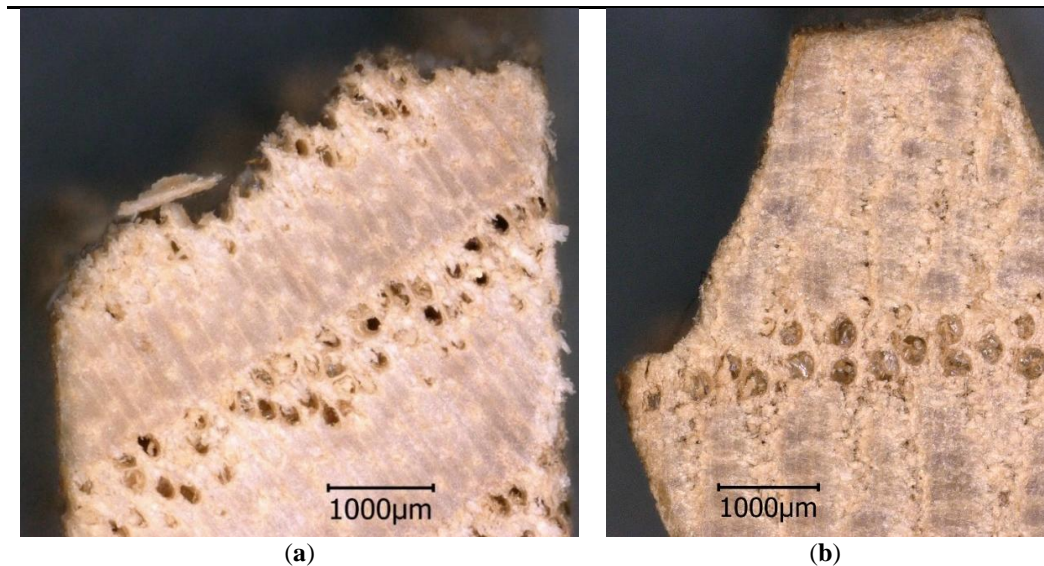


Figure 3. The fracture pattern in the ring-porous hardwoods: (a) Cross section of the Ash, fracture within a ring of the earlywood vessels; (b) Cross section of the English oak heartwood, fracture along the field of the latewood pores and the adjacent parenchyma cells.

By far, the Sweet chestnut showed the lowest RIM among the ring-porous hardwoods, which might be related to its high wood ray density (Table 4), but no clear correlation between the ray density and structural integrity became evident (Figure 4). Furthermore, the radial fractures in the Sweet chestnut were also running from one vessel to the next. More likely, the higher percentage of vessels and axial parenchyma leads to a higher number of weak points within the xylem of the Sweet chestnut compared to the other ring-porous species within this study.

The group of semi-ring-porous hardwood species, which was represented by the Teak, Wild cherry and Walnut in this study, takes an intermediate position between the ring- and the diffuse-porous species. This also became evident when analyzing the fracture patterns obtained through the HEMI-test. As shown in Figure 5a for the Wild cherry, the fractures occurred along the growth ring borders but did not run through the earlywood vessel rings.

In the diffuse-porous hardwoods, the RIM varied most, i.e., between 80.9% (Kiri) and 90.3% (Boxwood), respectively. Although these two species also represent the extremes in ODD, the latter was not correlated with the structural integrity, as shown in Figure 1. Nevertheless, in contrast to the ring-porous hardwood species, the average earlywood vessel diameter of the diffuse-porous hardwood species was correlated with the RIM ($R^2 = 0.4704$), as shown in Figure 6. [12] studied angiosperm wood species and concluded that the tissue density outside the vessel lumens must predominantly influence wood density. Furthermore, they suggest that both the density and the vessel lumen fraction affect the mechanical strength properties.

It became also obvious that in different wood species such as the Kiri, Walnut, Shining gum and further tropical species, the fractures occurred between the vessels, both in the radial and tangential directions (Table 4). Consequently, the vessels turned out to be general weak points in the fiber tissue of the hardwoods, where the weakness increases with an increasing vessel diameter. Figure 7a shows, as an example for the Bongossi, that the vessels served as a starting point for the fractures independently from its anatomical orientation. Tropical species with comparatively small vessels such as the Amaranth, Bangkirai, Garapa, and Ipé showed a rather high RIM. On the extreme end of

the scale, the Merbau showed the lowest RIM and also the largest vessel diameters of all the species. Furthermore, distinct parenchyma bands and wood rays appeared to be weak (and therefore starting points for fractures) in tropical species as well, as also shown in Figure 7. The fractures cutting the wood rays appeared only where the rays were deflected by the vessels from their straight radial orientation.

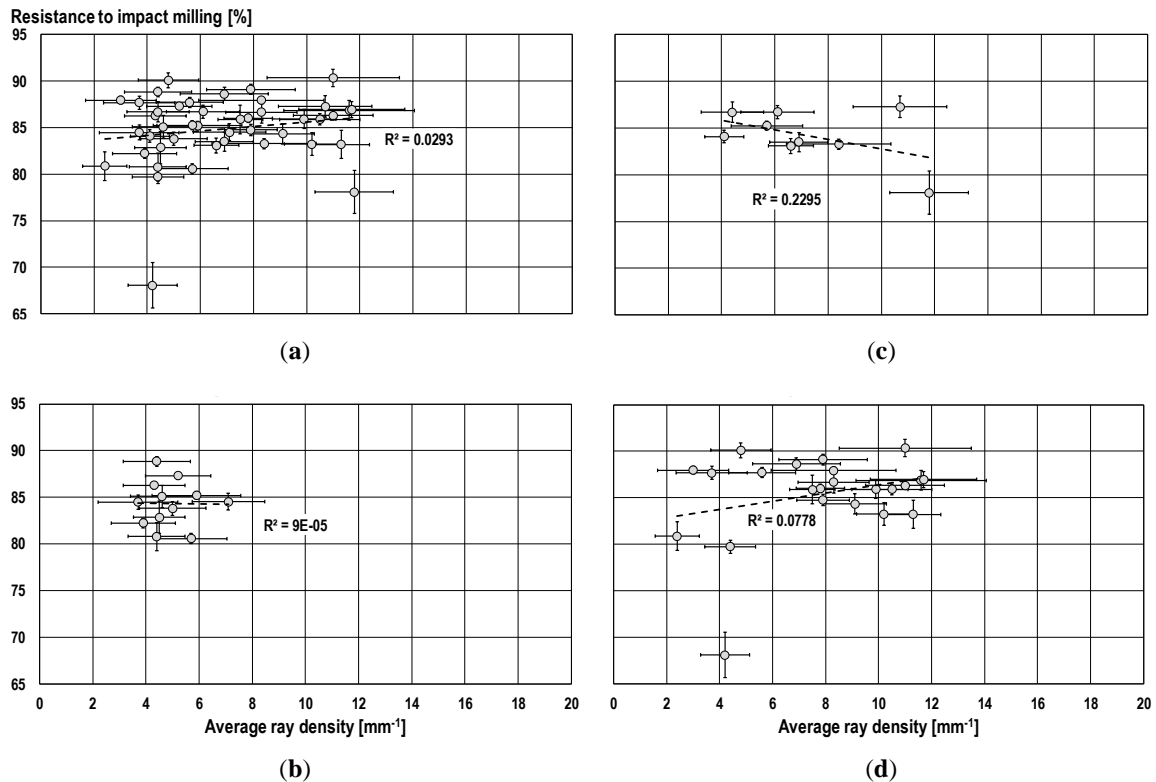


Figure 4. The relationship between the average ray density and the Resistance to Impact Milling (RIM): (a) all wood species ($y = 0.2354x + 83.247$); (b) softwoods ($y = -0.0252x + 84.454$); (c) ring- and semi-ring-porous hardwoods ($y = -0.5083x + 87.875$); (d) and diffuse-porous hardwoods ($y = 0.4365x + 81.997$).

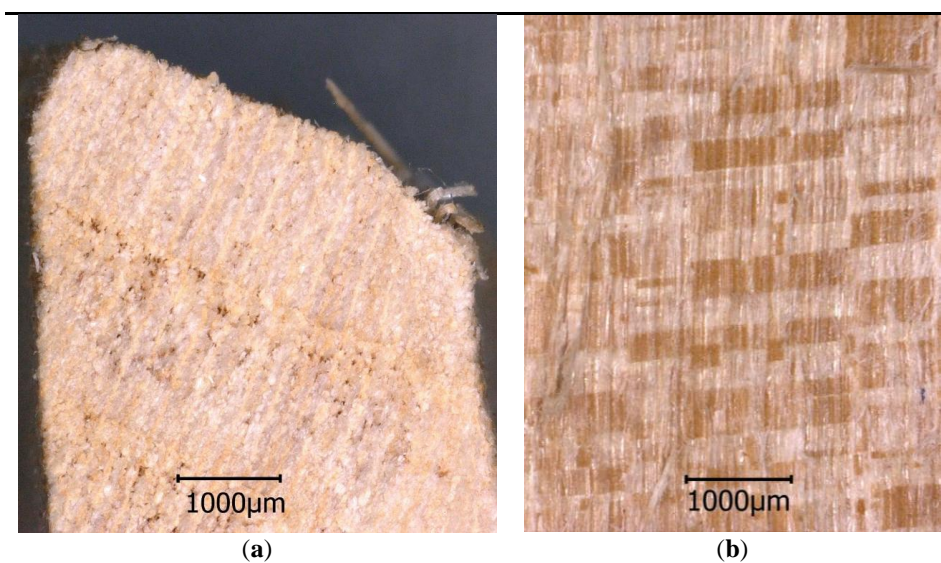


Figure 5. The fracture pattern in semi-ring-porous and diffuse-porous hardwoods: (a) the cross section of the Wild cherry, the fracture along a growth ring border; (b) the radial fracture section of the Alder, the fracture along the rays.

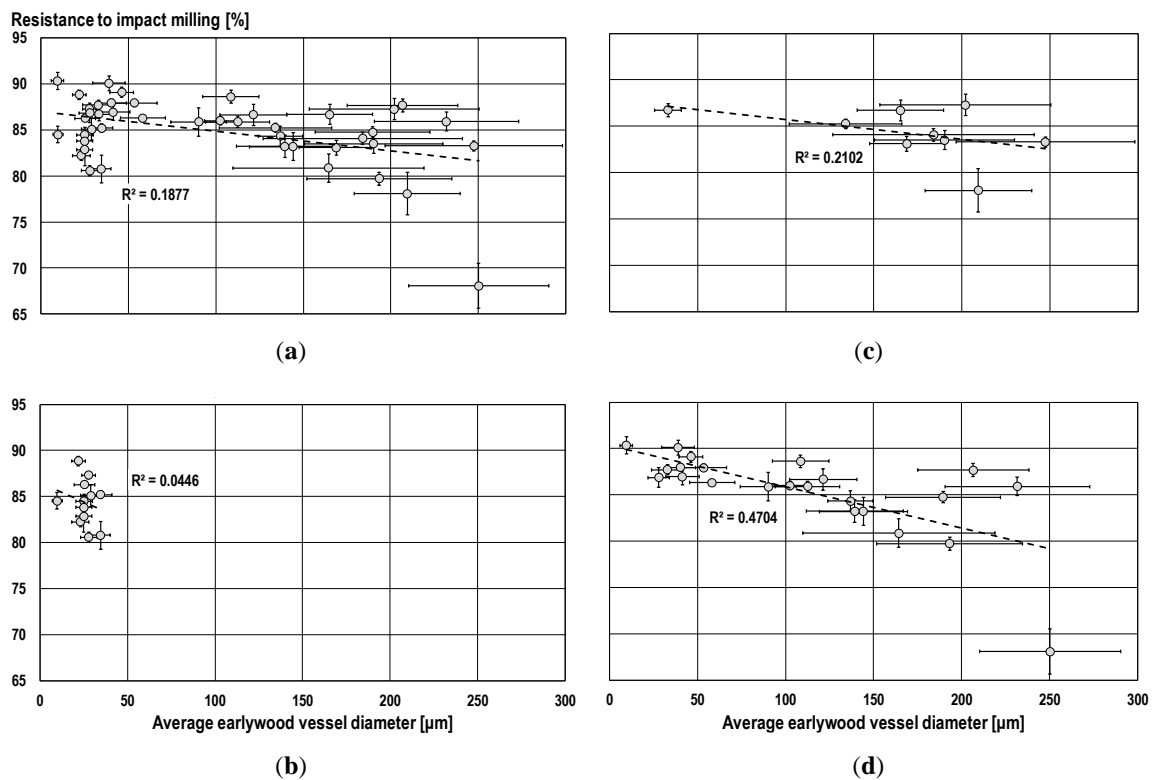


Figure 6. The relationship between the average earlywood vessel diameters and the resistance to impact milling (RIM): (a) all wood species ($y = -0.0213x + 86.982$); (b) softwoods ($y = -0.0814x + 86.425$); (c) ring- and semi-ring-porous hardwoods ($y = -0.0213x + 87.857$); and (d) diffuse-porous hardwoods ($y = -0.0445x + 90.309$).

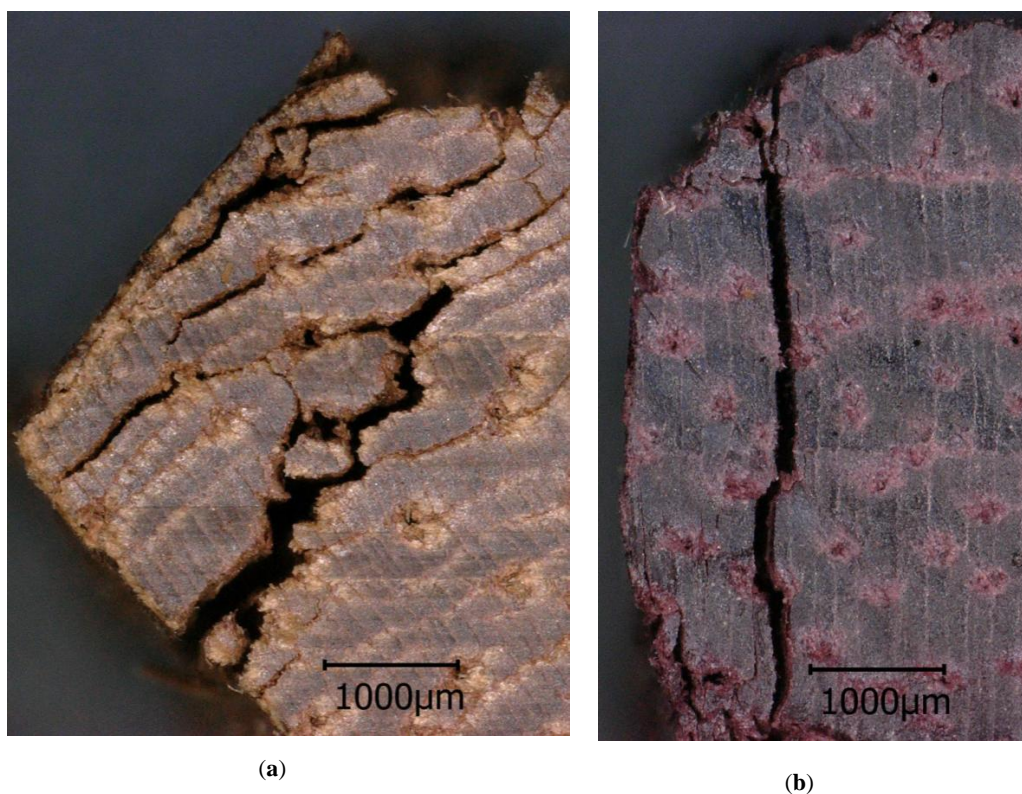


Figure 7. The fracture pattern in the diffuse-porous hardwoods: (a) the cross section of the Bongossi, the tangential fractures; (b) the cross section of the Amaranth—the radial fractures along the rays.

4. Conclusions

In this study, we showed that the differences in the structural integrity of wood and thus in the brittleness are predominantly affected by anatomical characteristics. The size, density and distribution of the vessels as well as the ray density of the wood were found to have a significant impact on the structural integrity of the hardwoods. The structural integrity of the softwoods was, on the other hand, affected by the number of growth ring borders and the occurrence of resin canals. The density affected the Resistance to Impact Milling (RIM) of neither the softwoods nor the hardwoods.

Consequently, for applications where the brittleness of wood is more relevant than its elasto-mechanical properties, which are generally strongly correlated with wood density, other anatomical characteristics need to be considered for assessing wood quality. In particular, where dynamic loads impact on wooden components, the brittleness of wood becomes a critical issue. Dynamic loads paired with long-term wear and abrasion can be expected, for instance, on outdoor flooring. Furthermore, during wood processing, machining and handling during industrial processes, numerous dynamic impacts occur and affect the structural integrity of wood.

Wood quality is consequently strongly purpose-specific and cannot be simply derived from wood density data. Anatomical features showed a high potential to serve as better indicators for the structural integrity of wood. Additional influences such as the occurrence of reaction wood, alternating rotational growth and other types of fiber deviations likely affect the structural integrity of wood to a similarly extent. In summary, the findings from this study confirmed the need for test methods other than standard strength tests. As long as the common knowledge about wood anatomy and its effects on mechanical wood properties is incomplete, methods are needed that are sensitive, reliable, and accurate enough to characterize the structures of wood in a comprehensive manner. As shown with the HEMI-method applied in this study, indicators can be delivered for instance of the structural integrity of wood. However, further tests are needed, paired with more detailed analyses of the anatomical and chemical constitution of the wood samples being tested, to achieve a fully satisfactory insight on the relationship between wood anatomy and its structural integrity.

Author Contributions: Mainly responsible for the conceptualization, methodology used for these investigations and also the data evaluation, data validation and formal analysis was L.E. together with C.B. Investigations and data curation were conducted by G.W. together with L.E. The original draft of this article was prepared by L.E. together with C.B. who was involved in the review and editing process of this article. L.E. and G.W. did care for the visualization, supervised by C.B. who had the project's administration.

Funding: This research received no external funding.

Acknowledgments: The authors gratefully acknowledge Florian Zeller (GD Holz, Germany), Uwe Herrmann (Vandecasteele Houtimport, Belgium), Miha Humar (University Ljubljana, Slovenia) and Martin Rosengren (Rönnerum, Sweden) for providing wood samples.

Conflicts of Interest: The authors declare no conflict of interest.

References

1. Ghelmeziu, N. Untersuchungen über die Schlagfestigkeit von Bauhölzern. *Holz Roh. Werkst.* **1938**, *1*, 585–601. [[CrossRef](#)]
2. Beery, W.H.; Ifju, G.; McLain, T.E. Quantitative wood anatomy—Relating anatomy to transverse tensile strength. *Wood Fiber Sci.* **1983**, *15*, 395–407.
3. Alteyrac, J.; Cloutier, A.; Ung, C.H.; Zhang, S.Y. Mechanical properties in relation to selected wood characteristics of black spruce. *Wood Fiber Sci.* **2007**, *38*, 229–237.
4. Rapp, A.O.; Brischke, C.; Welzbacher, C.R. Interrelationship between the severity of heat treatments and sieve fractions after impact ball milling: A mechanical test for quality control of thermally modified wood. *Holzforschung* **2006**, *60*, 64–70. [[CrossRef](#)]
5. Brischke, C. Agents affecting the structural integrity of wood. In Proceedings of the 10th Meeting of the Northern European Network on Wood Science and Engineering, Edinburgh, UK, 13–14 October 2014; pp. 43–48.

6. Zimmer, K.; Brischke, C. Within-species variation of structural integrity—A test on 204 Scots pine trees from Northern Europe. In Proceedings of the 12th Meeting of the Northern European Network on Wood Science and Engineering, Riga, Latvia, 12–13 September 2016.
7. Brischke, C. Interrelationship between static and dynamic strength properties of wood and its structural integrity. *Drvna Ind.* **2017**, *68*, 53–60. [[CrossRef](#)]
8. Brischke, C.; Rapp, A.O.; Welzbacher, C.R. High-energy multiple impact (HEMI)-test—Part1: A new tool for quality control of thermally modified timber. In Proceedings of the The International Research Group on Wood Preservation, Tromsø, Norway, 18–22 June 2006; IRG Document No: IRG/WP/06-20346.
9. ISO 5223. *Test Sieves for Cereals*; ISO (International Organization for Standardization): Geneva, Switzerland, 1996.
10. Reiterer, A.; Burgert, I.; Sinn, G.; Tschegg, S. The radial reinforcement of the wood structure and its implication on mechanical and fracture mechanical properties—a comparison between two tree species. *J. Mater. Sci.* **2002**, *37*, 935–940. [[CrossRef](#)]
11. Bamber, R.K. Sapwood and heartwood. In *Forestry Commission of New South Wales; Wood Technology and Forest Research Division: Beecroft, Australia, 1987; Volume 2*, pp. 1–7.
12. Zanne, A.E.; Westoby, M.; Falster, D.S.; Ackerly, D.D.; Loarie, S.R.; Arnold, S.E.J.; Coomes, D.A. Angiosperm wood structure: Global patterns in vessel anatomy and their relation to wood density and potential conductivity. *Am. J. Bot.* **2010**, *97*, 207–215. [[CrossRef](#)] [[PubMed](#)]



© 2019 by the authors. Licensee MDPI, Basel, Switzerland. This article is an open access article distributed under the terms and conditions of the Creative Commons Attribution (CC BY) license (<http://creativecommons.org/licenses/by/4.0/>).